INTERNATIONAL JOURNAL FOR NUMERICAL METHODS IN FLUIDS, VOL. 11, 21–38 (1990)

TAYLOR–LEAST-SQUARES FINITE ELEMENT FOR TWO-DIMENSIONAL ADVECTION-DOMINATED UNSTEADY ADVECTION–DIFFUSION PROBLEMS

NAM-SIK PARK* AND JAMES A. LIGGETT

School of Civil and Environmental Engineering, Cornell University, Ithaca, NY 14853 U.S.A.

SUMMARY

A new finite element method, the Taylor–least-squares, is proposed to approximate the advection-dominated unsteady advection–diffusion equation. The new scheme is a direct generalization of the Taylor–Galerkin and least-squares finite element methods. Higher-order spatial derivatives in the new formulation necessitate higher-degree polynomials. Hermite cubic shape functions are used. Extensive comparisons with other methods in one dimension proved that the new scheme is a step forward in modelling this difficult problem. The method offers straightforward generalizations to higher dimensions without losing the accuracy demonstrated in one dimension, i.e. the method preserves the important property of the Taylor–Galerkin scheme of being free of numerical crosswind diffusion. Several numerical experiments were made in two dimensions and excellent results were obtained from the representative experiments.

KEY WORDS Advection Diffusion Finite element Two-dimensional

1. INTRODUCTION

It is well known that the conventional numerical approximations of the advection–diffusion equation produce infamous spurious oscillations and/or numerical diffusion when advection dominates. Price *et al.*[1] found that spurious oscillations occur when a centred finite difference approximation is used with a grid Peclet number greater than two. Later, Jensen and Finlayson[2] showed that for various finite element approximations the upper limit of the grid Peclet number ranged from two to five if spurious oscillations are to be avoided. The difficulty of satisfying such criteria is that the grid becomes unrealistically fine, approaching a zero grid spacing for a hyperbolic system which has no diffusion.

To reduce spurious oscillations and/or numerical dissipation, various methods were proposed. Some of them offered very accurate solutions. Examples are the von Rosenberg method[3] which is essentially a Peclet-number-weighted average of the backward and centred differences of the advection term for the unit Courant number, the piecewise parabolic method by Colella and Woodward[4] who used a higher-order Godunov method[5] to improve resolutions of jumps, the characteristic finite element method by Varoglu and Finn,[6] etc. Unfortunately, the above schemes cannot be directly applied to multidimensions and/or lose accuracy in higher dimensions.[7]

* Currently at HydroGeoLogic, Inc., 503 Carlisle Dr., Suite 250, Herndon, VA 22070, U.S.A.

0271–2091/90/090021–18$09.00

Received 28 December 1988
Revised 12 May 1989

Computationally, an adaptive scheme[8,9] can be efficient but cannot be used for pure advection problems.[8] Petrov–Galerkin schemes have been studied a great deal since the work of Christie *et al.*[10] Multidimensional Petrov–Galerkin schemes have been improved by Hughes and Brooks[11] to reduce crosswind diffusion. The Petrov–Galerkin methods have been further improved by Galeão and Dutra Do Carmo[12] and Franca *et al.*[13] among others.

One of the favourite methods in multidimensions is the fractional time step operator-splitting method.[14–17] The idea is to treat the advection and dispersion parts separately in each fractional time step and use different numerical schemes for different physical processes. The crucial part of this scheme is the advection step and the method of characteristics is a natural choice. The accuracy of the method of characteristics depends largely on the interpolation scheme. In the earlier studies previously mentioned, a cubic polynomial was used for interpolation at the foot of characteristics, thereby greatly reducing the error associated with a linear interpolation. In spite of the good results, the operator-splitting methods have the weakness that the downstream boundary condition cannot be satisfied during the advection time steps, though it can be shown that the error in the boundary value is first-order in time.[18]

Another good multidimensional scheme is based on higher-order time approximations. Morton and Parrott[19] considered the problem of a proper coupling between the time discretization and the Galerkin spatial approximation of hyperbolic problems, noting that the Galerkin spatial approximation is fourth-order accurate. Donea *et al.*[20,21] developed the Taylor–Galerkin method which is third-order accurate in time. The Taylor–Galerkin method has all the advantages of the Petrov–Galerkin methods while allowing straightforward generalizations to higher dimensions. On the other hand, Carey and Jiang[22] used least-squares finite elements for first-order hyperbolic systems. They showed that the semidiscretized equation of the least-squares method is very similar to that of the Taylor–Galerkin scheme.

An earlier study indicated that the use of a higher-order interpolation function such as the Hermite cubic polynomial yielded very accurate solutions for the advection of smooth profiles even if they were steep. However, for profiles with sharp fronts, the cubic elements gave worse results than linear elements when either the standard Galerkin or Taylor–Galerkin method was used. In this study a new finite element formulation is proposed which gives very accurate solutions for both cases. The new formulation, the Taylor–least-squares method, is based on the higher-order time approximation using the Taylor series and the least-squares methods. In the next section the Taylor–least-squares scheme is developed first for the one-dimensional advection equation. Then the amplitude and phase errors for the Taylor–Galerkin, least squares and Taylor–least-squares methods are examined. The accuracy of the Taylor–least-squares scheme is demonstrated by numerical examples.

Donea *et al.*[20] indicated that for the advection–diffusion equation only the second-order Taylor–Galerkin scheme is possible, owing to the presence of the diffusion term, unless an operator-splitting method is used. In this study the advection–diffusion equation is discretized with different accuracies for advection and diffusion operators so that third-order accuracy is recovered in the limit of zero diffusion. Finally, the multidimensional Taylor–least-squares method is derived and is applied in two dimensions to demonstrate its direct extension to higher dimensions and its accuracy.

2. THE TAYLOR–LEAST SQUARES FINITE ELEMENT METHOD

The one-dimensional scalar advection–diffusion equation in a homogeneous medium with an incompressible flow velocity is

$$(\partial_t + u\partial_x - D\partial_x^2)\, c = 0, \tag{1}$$

where u is the flow field, D is the diffusion coefficient, $t \in [0, \infty)$ and $x \in [x_0, x_N]$. Appropriate initial and boundary conditions constitute a well-posed problem. Numerical schemes suffer when diffusion is small compared to advection, so consider the extreme case, the equation for pure advection,

$$(\partial_t + u\partial_x)c = 0, \tag{2}$$

with a boundary condition at the inflow boundary and an initial condition. Donea *et al.*[21] developed the Lax–Wendroff Taylor–Galerkin (LWTG) and Crank–Nicolson Taylor–Galerkin (CNTG) schemes which are third- and fourth-order accurate in time respectively. Since the derivations of the Taylor–Galerkin and least-squares schemes are essential to the derivation of the new scheme, they will be reviewed briefly. The Taylor–Galerkin methods can be derived at once using the θ-weighted time discretization. Expand $c(x,(n+1)\Delta t)$ about $c(x, n\Delta t)$ and rewrite as

$$\frac{c^{n+1}-c^n}{\Delta t} = \partial_t c^n + \frac{\Delta t}{2}\partial_t^2 c^n + \frac{(\Delta t)^2}{6}\partial_t^3 c^n + O((\Delta t)^3), \tag{3}$$

where $c^n = c(x, n\Delta t)$. Conversely, expand $c(x, n\Delta t)$ about $c(x,(n+1)\Delta t)$ and rewrite to get

$$\frac{c^{n+1}-c^n}{\Delta t} = \partial_t c^{n+1} - \frac{\Delta t}{2}\partial_t^2 c^{n+1} + \frac{(\Delta t)^2}{6}\partial_t^3 c^{n+1} + O((\Delta t)^3). \tag{4}$$

A θ-weighted average of (3) and (4) is

$$\frac{c^{n+1}-c^n}{\Delta t} = \left(\partial_t + \frac{(\Delta t)^2}{6}\partial_t^3\right)[(1-\theta)c^n + \theta c^{n+1}] + \frac{\Delta t}{2}\partial_t^2[(1-\theta)c^n - \theta c^{n+1}] + O((\Delta t)^3). \tag{5}$$

Equation (5) is fourth-order accurate when $\theta = 1/2$ and is invariant with respect to the number of spatial dimensions since it only involves time derivatives. But from the one-dimensional advection equation,

$$\begin{aligned} \partial_t &= -u\partial_x, \\ \partial_t^2 &= u^2\partial_x^2, \\ \partial_t^3 &= u^2\partial_x^2\partial_t. \end{aligned} \tag{6}$$

The last substitution in (6) is necessary if linear elements are to be used. However, it turns out that the scheme becomes unstable for any value of θ when $-u^3\partial_x^3$ and cubic elements are used. Using (6) and a simple difference for the remaining time derivative one gets

$$\frac{c^{n+1}-c^n}{\Delta t} = -u\partial_x[(1-\theta)c^n + \theta c^{n+1}] + \frac{u^2\Delta t}{2}\partial_x^2\left[\left(\frac{2}{3}-\theta\right)c^n + \left(\frac{1}{3}-\theta\right)c^{n+1}\right]. \tag{7}$$

At this point it may be advantageous to introduce a local co-ordinate s to deduce an important parameter, the Courant number, and for the sake of shape functions which are more convenient in local co-ordinates. The local co-ordinate $s \in [-1, 1]$ is

$$s = \frac{2x - (x_i + x_{i+1})}{\Delta x}, \quad x \in [x_i, x_{i+1}],$$

where

$$\Delta x = x_{i+1} - x_i.$$

For $\theta=0$, (7) in local co-ordinates becomes

$$\left[1-\frac{2}{3}v^2\partial_s^2\right]\left(\frac{c^{n+1}-c^n}{\Delta t}\right)+[1-v\partial_s](u\partial_x c^n)=0, \tag{8}$$

where v is the Courant number ($u\Delta t/\Delta x$). Equation (8) is identical to the semidiscretized third-order accurate LWTG equation given by Donea *et al.*[21] For $\theta=1/2$ one gets

$$\left[1+v\partial_s+\frac{v^2}{3}\partial_s^2\right]\left(\frac{c^{n+1}-c^n}{\Delta t}\right)+u\partial_x c^n=0, \tag{9}$$

which is identical to the fourth-order accurate CNTG equation of Donea *et al.*[21]

Carey and Jiang[22] proposed the least-squares (LS) method for solutions of hyperbolic systems. Using the θ-weighted time difference, the LS functional of (2) is

$$I(t)=\int_{x_0}^{x_N}\mathrm{d}x\left[\frac{c^{n+1}-c^n}{\Delta t}+\theta u\partial_x c^{n+1}+(1-\theta)u\partial_x c^n\right]^2. \tag{10}$$

Taking a variation with respect to c^{n+1} and letting $\delta I(t)=0$,

$$\delta I(t)=2\int_{x_0}^{x_N}\mathrm{d}x\left[\frac{c^{n+1}-c^n}{\Delta t}+\theta u\partial_x c^{n+1}+(1-\theta)u\partial_x c^n\right]\left[\left(\frac{1}{\Delta t}+\theta u\partial_x\right)\delta c^{n+1}\right]=0 \tag{11}$$

Identifying δc^{n+1} as a weighting function w and after an integration by parts, the Euler equation in local co-ordinates becomes

$$[1-v^2\partial_s^2]\left(\frac{c^{n+1}-c^n}{\Delta t}\right)+[1-v\partial_s](u\partial_x c^n)=0, \tag{12}$$

in which θ has been replaced by 1/2. The LS equation (12) is very similar to the LWTG equation (8) except that the coefficient $-2/3$ is replaced by -1.

The Taylor–least-squares (TLS) formulation is obtained similarly. First, the advection equation is discretized in time up to third-order and then a least-squares functional is formed from the semidiscretized equation. Using the third-order accurate equation (7) inside the square brackets in (10), the least-squares functional for the TLS scheme is obtained as

$$I(t)=\int_{x_0}^{x_N}\mathrm{d}x\left\{\frac{c^{n+1}-c^n}{\Delta t}+u\partial_x[(1-\theta)c^n+\theta c^{n+1}]-\frac{u^2\Delta t}{2}\partial_x^2\left[\left(\frac{2}{3}-\theta\right)c^n+\left(\frac{1}{3}-\theta\right)c^{n+1}\right]\right\}^2. \tag{13}$$

The final TLS formula results by equating the variation of the functional to zero. The scheme is third-order in general and is fourth-order for $\theta=1/2$. The Euler equation for the fourth-order TLS scheme is

$$\left[1-\frac{v^2}{3}\partial_s^2+\frac{v^4}{9}\partial_s^4\right]\left(\frac{c^{n+1}-c^n}{\Delta t}\right)+\left[1-v\partial_s+\frac{v^2}{3}\partial_s^2\right](u\partial_x c^n)=0. \tag{14}$$

The fourth-order spatial derivative results from integrating $\delta I(t)$ by parts twice. The first two terms in the square brackets in (14) are similar to those of (8) and (12) except for the coefficient of $-1/3$, but it will be shown that improvements in numerical experiments due to the coefficient and the extra terms are rather significant. According to Morton,[24] all the Euler equations can be interpreted as having different mixed norms for approximations of advection and diffusion terms.

The Euler equations for the LWTG, CNTG, TLS and LS schemes can now be further discretized by appropriate shape functions. Obviously the conventional linear ('hat') function

cannot be used for the TLS scheme owing to the higher-order derivatives. For the TLS scheme the Hermite cubic polynomial (e.g. Reference 25) is chosen. The shape functions in local co-ordinates are

$$c(s,t) = c_i(t)N_1(s) + \frac{\partial c_i}{\partial x}(t)N_2(s) + c_{i+1}(t)N_3(s) + \frac{\partial c_{i+1}}{\partial x}(t)N_4(s), \tag{15}$$

where

$$N_1 = \tfrac{1}{4}(s-1)^2(s+2), \qquad N_2 = (\Delta x/8)(s-1)^2(s+1),$$
$$N_3 = -\tfrac{1}{4}(s+1)^2(s-2), \qquad N_4 = (\Delta x/8)(s+1)^2(s-1).$$

For other schemes both linear and the cubic elements are used. In the next section Fourier analysis is used to examine the accuracy characteristics of the various methods.

3. FOURIER ANALYSIS

Certain accuracy characteristics of a numerical scheme can be examined by Fourier analysis. Numerical eigenvalues are obtained by substituting a Fourier mode e^{ikx}, where k is a wave number and $i = \sqrt{(-1)}$, into the fully discretized equations. For LWTG with the linear element[21]

$$\xi^1_{LW} = 1 - \frac{2\nu^2 \sin^2(k\Delta x/2) + i\nu \sin(k\Delta x)}{1 - \frac{2}{3}(1-\nu^2)\sin^2(k\Delta x/2)}. \tag{16}$$

For LS with the linear element[22]

$$\xi^1_{LS} = 1 - \frac{4\theta\nu^2 \sin^2(k\Delta x/2) + i\nu \sin(k\Delta x)}{1 - 4(\frac{1}{6} - \theta^2\nu^2)\sin^2(k\Delta x/2)}. \tag{17}$$

For the LWTG, LS and TLS schemes with the cubic elements, all eigenvalues have same form as

$$\xi^c = \frac{-b \pm \sqrt{(b^2 - 4ad)}}{2a}, \tag{18}$$

where a, b and d for each method can be found in the Appendix. In general, the amplification factor ξ is complex and $c^{n+1} = \xi c^n$. The analytic eigenvalue for the continuum equation (2) is

$$\xi_a = e^{-iku\Delta t}. \tag{19}$$

Note that because one continuum equation is approximated by two discrete equations, one for the primary unknown and the other for its derivative, there are two eigenvalues, physical and computational, associated with a numerical scheme when the cubic element is used.[26]

One way of measuring the accuracy of a numerical scheme is to compare the modulus and argument of a numerical eigenvalue to those of the continuum eigenvalue. For the amplitude error define

$$R = \frac{|\xi|}{|\xi_a|} = |\xi|, \tag{20}$$

since $|\xi_a| = 1$, and for the phase error

$$\Phi = \frac{\arg(\xi)}{\arg(\xi_a)} = -\frac{\tan^{-1}[\mathrm{Im}(\xi)/\mathrm{Re}(\xi)]}{\nu k \Delta x}. \tag{21}$$

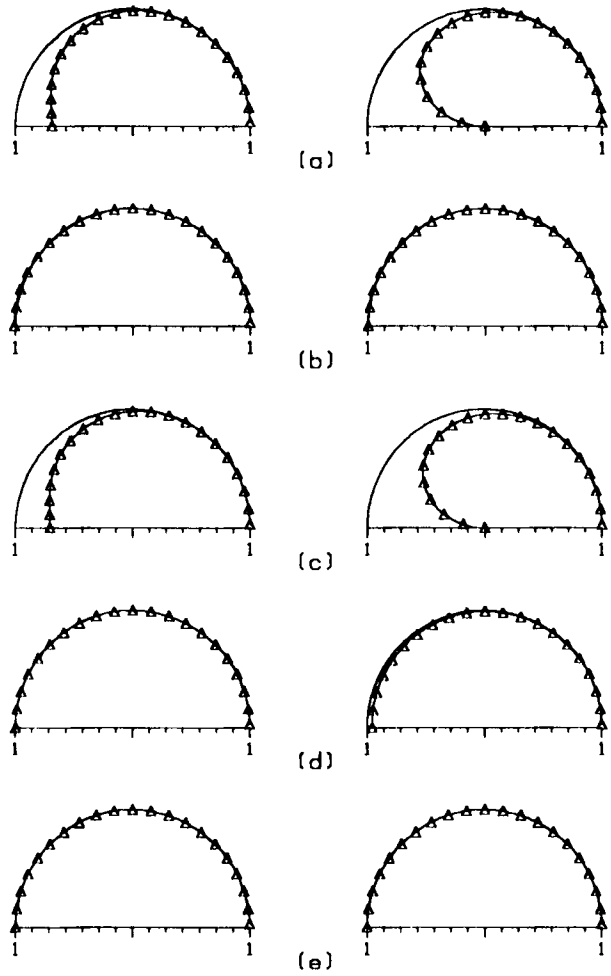

Figure 1. Relative amplitude (left column) and phase (right column) errors for $\nu = 0{\cdot}24$: (a) linear LWTG; (b) cubic LWTG; (c) linear LS; (d) cubic LS; (e) TLS; ——, analytic; —Δ—, numerical

Table I. Comparison of L^2-error of Fourier analyses for various methods

	Linear LWTG	Cubic LWTG	Linear LS	Cubic LS	TLS
ε_R	1·28	$0{\cdot}362 \times 10^{-1}$	1·24	$0{\cdot}344 \times 10^{-2}$	$0{\cdot}428 \times 10^{-2}$
ε_Φ	3·15	$0{\cdot}168 \times 10^{-1}$	3·27	0·198	$0{\cdot}245 \times 10^{-2}$

Polar plots of the amplitude and phase errors are given in Figure 1, and the discrete L^2-error (ξ), measured by (22) with a normalization factor of unity, is given in Table I:

$$\varepsilon = \left(\sum_{j=1}^{N} (1-\gamma_j)^2 \right)^{1/2}, \tag{22}$$

where γ_j is a discrete value of either R or Φ, and N is the total number of discrete points. The Fourier analysis for the fourth-order accurate CNTG is not reported here owing to its poor performance. The scheme gives much worse spurious oscillations than the LWTG scheme although it has the least amplitude and phase errors: it is non-dissipative (zero amplitude error) and has the smallest phase error among the methods tested in this report. The linear LWTG and linear LS schemes behave quite similarly, as shown in Figures 1(a) and 1(c) and in Table I. The error plots for the cubic elements are considerably better than for linear elements and the differences among them appear to be small, although the TLS scheme is marginally better than the others. However, numerical experiments in the next section show that the marginal improvement makes a rather large computational difference.

4. NUMERICAL EXAMPLES

Two one-dimensional example problems were chosen from Reference 27 which set a number of specific problems as tests of the performance of numerical solutions of the advection–diffusion equation. They are pure advection of a Gaussian hill and of a sharp front. For the Gaussian hill the prescribed conditions are

$$c(x,0) = \exp\left(-\frac{(x-2000)^2}{2\sigma^2}\right)$$

and

$$c(0,t) = 0,$$

where $\sigma = 264$ and $x \in [0, 12\,800]$. The hill is steep in the sense that the hill decreases to 1% of the peak value over $4\Delta x$. For the second problem the initial and boundary conditions are

$$c(x,0) = 0$$

and

$$c(0,t) = 1.$$

Parameters common to both problems are: uniform spatial discretization of $\Delta x = 200$, constant flow velocity ($u = 0{\cdot}5$), time step $\Delta t = 96$ and the solutions are examined at $t = 9600$. It is difficult for one numerical scheme to model both examples well. In particular with both linear and the cubic elements, the CNTG scheme, which has the best accuracy based on the Fourier analysis, gives excellent results for the Gaussian hill problem but poor results for the sharp front problem. Thus small dissipation in amplitude can be advantageous to dampen error due to incorrect phase transport. The LWTG and LS schemes are tested along with linear and the cubic elements, and the TLS scheme is tested with the cubic elements. The results are reported in Figure 2. As was expected from the Fourier analyses, the two schemes with linear elements yield similar results (Figure 2(a) and 2(c)). All three schemes with the cubic elements perform well for the Gaussian hill problem. However, for the sharp front problem, the LWTG and LS schemes give worse results than their linear counterparts. But the result from the TLS scheme is far better than those of the others: the front is distributed only over $5\Delta x$ compared to $8\Delta x - 10\Delta x$ for other schemes, including that of Ding and Liu.[16]

The performance of the TLS scheme for other values of θ and ν is given in Figure 3. Figure 3 shows the example problems with $\nu = 0{\cdot}5$ ($\Delta t = 100$), $\theta = 0{\cdot}5$ and $\nu = 1{\cdot}0$ ($\Delta t = 200$), $\theta = 1{\cdot}0$. The scheme fails to provide useful solutions for the following combinations: $\theta = 0$, $\nu = 0{\cdot}5$ and $\theta = 0, 0{\cdot}5$, $\nu = 1$. The results from $\nu = 0{\cdot}5$, $\theta = 0{\cdot}5$ are very good, but when the Courant number is extended to

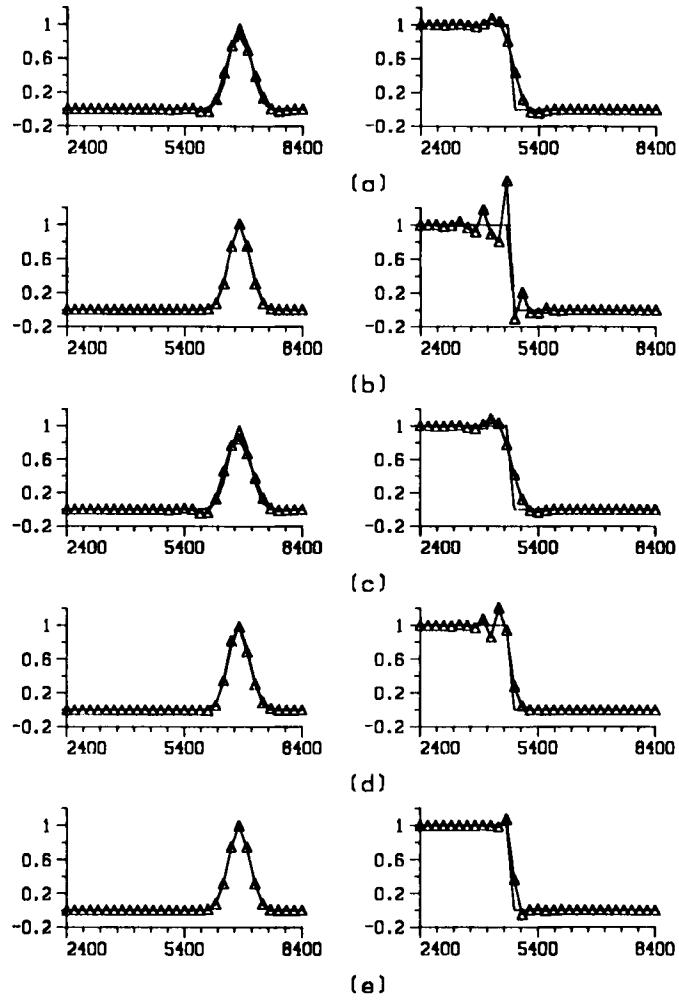

Figure 2. Pure advection of the Gaussian hill and the sharp front: (a) linear LWTG; (b) cubic LWTG; (c) linear LS; (d) cubic LS; (e) TLS; ——, analytic; —Δ—, numerical

unity the solution degrades. Unfortunately, a stability relationship between v and θ cannot be obtained owing to the complexity of the numerical eigenvalues.

5. HIGHER-ORDER APPROXIMATION OF THE ADVECTION–DIFFUSION EQUATION

As was shown in the previous section, higher-order time approximations imply higher-order spatial derivatives. Therefore the straight application of the Taylor–Galerkin scheme to the advection–diffusion equation allows only second-order accuracy in time. However, with the use of the fractional time step operator-splitting method, one can retain higher-order accuracies for the advection part.[20] If the advection and diffusion equations are solved separately, violation of the downstream boundary condition is inevitable during the advection step. In this study the

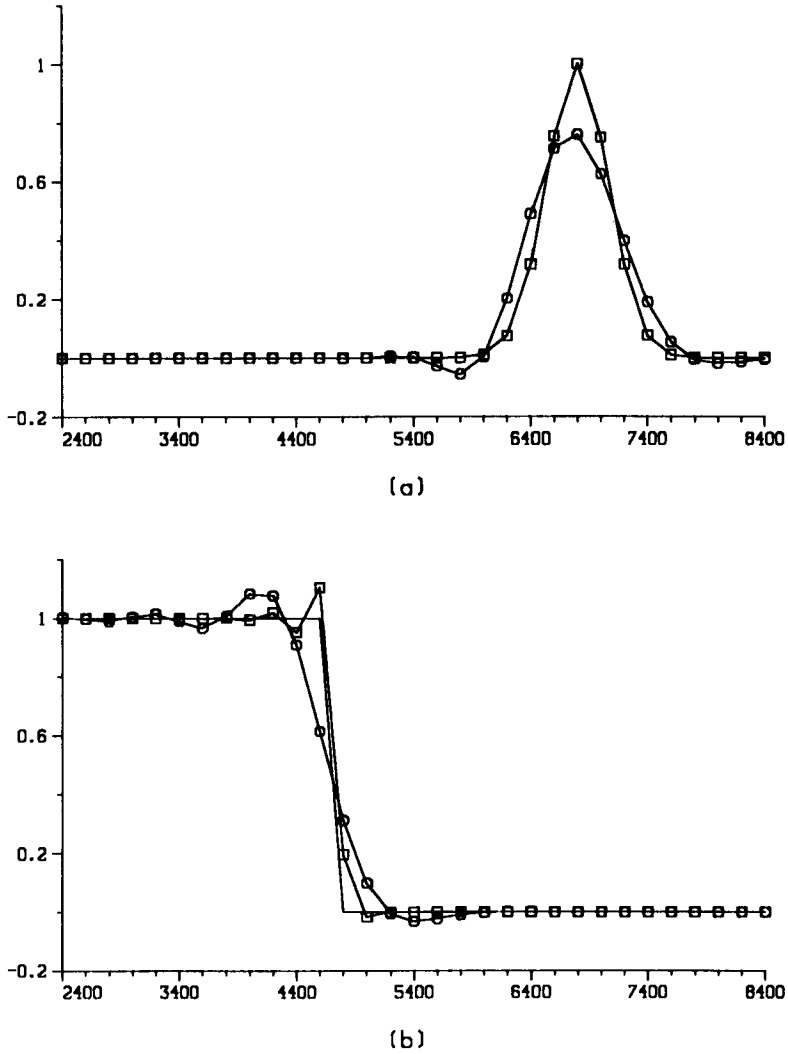

Figure 3. The TLS scheme for other values of θ and v: ——, analytic, —□—, $\theta = 0{\cdot}5$, $v = 0{\cdot}5$; —○—, $\theta = 1$, $v = 1$

operator-splitting method is employed to use the higher-order approximation for the advection operator, but the two equations are never solved separately. It is done by formally adding the two semidiscrete equations with possibly different accuracies and fully discretizing the resulting equation using the least-squares procedure. This way one can avoid violating the downstream boundary condition at any time. Following Donea *et al.*,[20] the advection part becomes

$$(\partial_t + u\partial_x)c_1 = 0 \tag{23}$$

and for the diffusion

$$(\partial_t - D\partial_x^2)c_2 = 0, \tag{24}$$

where $c_1^n = c^n$, $c_2^n = c_1^{n+1}$ and $c^{n+1} = c_2^{n+1}$. The third-order approximation of (23) is (7) with the

subscript 1:

$$\frac{c_1^{n+1}-c_1^n}{\Delta t} = -u\partial_x[(1-\theta)c_1^n + \theta c_1^{n+1}] + \frac{u^2\Delta t}{2}\partial_x^2\left[\left(\frac{2}{3}-\theta\right)c_1^n + \left(\frac{1}{3}-\theta\right)c_1^{n+1}\right]. \tag{25}$$

For the well-behaved diffusion part, the Crank–Nicolson method is used:

$$\frac{c_2^{n+1}-c_2^n}{\Delta t} = \frac{D}{2}\partial_x^2[c_2^{n+1} + c_2^n]. \tag{26}$$

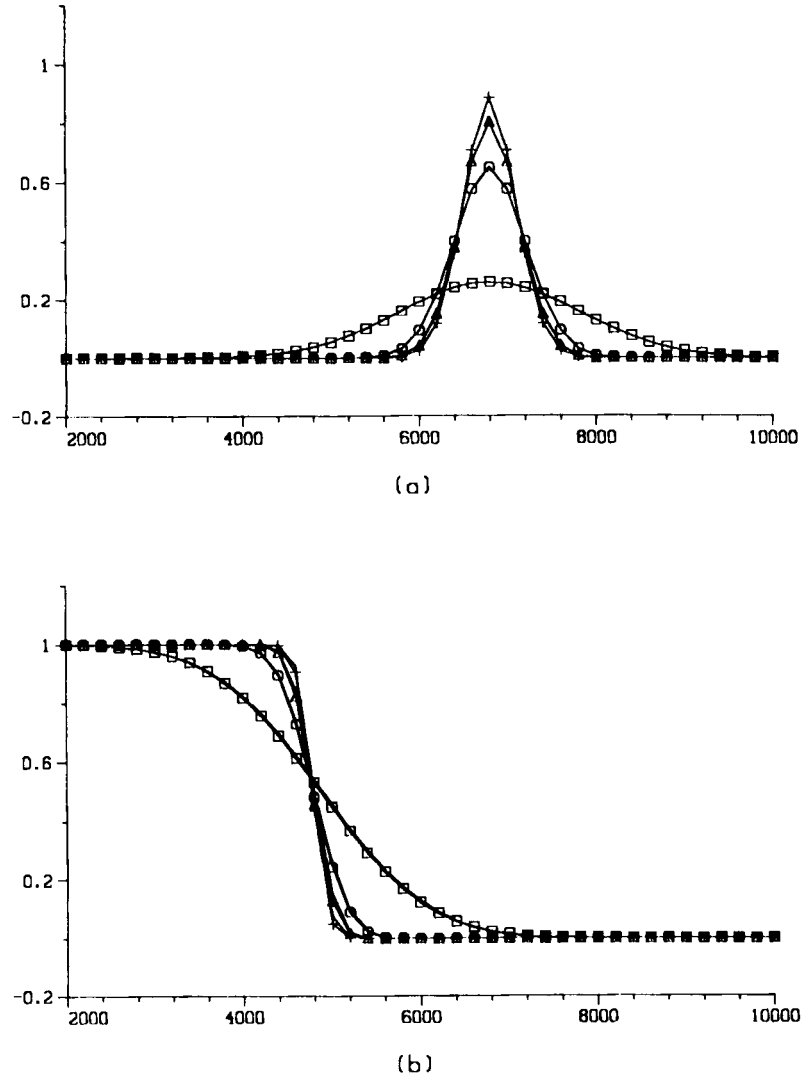

Figure 4. Results of the TLS scheme for the advection–diffusion equation with various Peclet numbers: ——, analytic; — + — $P_e = 100$, —△—, $P_e = 50$; —○—, $P_e = 20$; —□—, $P_e = 2$

Adding (25) and (26) gives

$$\frac{c_2^{n+1}-c_1^n}{\Delta t} = -u\partial_x[(1-\theta)c_1^n + \theta c_1^{n+1}] + \frac{u^2\Delta t}{2}\partial_x^2\left[\left(\frac{2}{3}-\theta\right)c_1^n + \left(\frac{1}{3}-\theta\right)c_1^{n+1}\right] + \frac{D}{2}\partial_x^2[c_2^{n+1}+c_2^n]. \tag{27}$$

To remove the intermediate values c_2^n and c_1^{n+1}, the Taylor series is used. In the advection part c_1^{n+1} is expanded about c_2^{n+1} and in the diffusion part c_2^n is expanded about c_1^n. Switching back to the original variables, the semidiscretized equation becomes

$$\frac{c^{n+1}-c^n}{\Delta t} = -u\partial_x[(1-\theta)c^n + \theta c^{n+1}] + \frac{1}{2}\partial_x^2\left[\left(D + u^2\Delta t\left(\frac{2}{3}-\theta\right)\right)c^n + \left(D + u^2\Delta t\left(\frac{1}{3}-\theta\right)\right)c^{n+1}\right]. \tag{28}$$

Thus first the advection–diffusion equation is split into two parts and then the two equations are discretized independently with different accuracies. As with the conventional operator-splitting method, there is an advantage in having different numerical schemes for different physical processes. Therefore the highly accurate TLS scheme can be retained for the advection part and the conventional second-order accurate Crank–Nicolson scheme can be used for the well-behaved diffusion part. The two semidiscrete equations are then added to avoid violating the downstream boundary condition. Then the intermediate values are removed using the Taylor series. The last process guarantees the recovery of third- or second-order accuracy for pure advection or pure diffusion respectively. Note, however, that when both advection and diffusion are present, the theoretical accuracy of the scheme is only $O(\Delta t)$ owing to the Taylor series substitutions into (28). Nevertheless, the numerical experiments showed no signs of degeneracy. The example problems in the previous section were calculated with various values of diffusion added. The results for Peclet ($u\Delta x/D$) numbers of 100, 50, 20 and 2 are given in Figure 4 and are in good agreement with the analytical solutions.

6. MULTIDIMENSIONAL TAYLOR–LEAST SQUARES SCHEME

The TLS scheme can be extended to higher dimensions without difficulty. The advection–diffusion equation is

$$[\partial_t + \mathbf{u}\cdot\nabla - \nabla\cdot(\mathbf{D}\cdot\nabla)]c = 0, \tag{29}$$

where $\mathbf{u}$ is the velocity vector, $\mathbf{D}$ is the diffusion tensor and ∇ is the gradient operator. The fractional time step method allows separate discretizations of the advection and diffusion parts. The third-order time approximation of the advection equation is the same as (5), but the substitutions for the time derivatives in higher dimensions become

$$\begin{aligned} \partial_t &= -\mathbf{u}\cdot\nabla, \\ \partial_t^2 &= \mathbf{uu}:\nabla\nabla + [(\mathbf{u}\cdot\nabla)\mathbf{u}]\cdot\nabla, \\ \partial_t^3 &= \{\mathbf{uu}:\nabla\nabla + [(\mathbf{u}\cdot\nabla)\mathbf{u}]\cdot\nabla\}\partial_t, \end{aligned} \tag{30}$$

where : is the scalar product of dyads. For the diffusion part the Crank–Nicolson method is used:

$$\frac{c^{n+1}-c^n}{\Delta t} = \tfrac{1}{2}[\nabla\cdot(\mathbf{D}\cdot\nabla)](c^{n+1}+c^n). \tag{31}$$

Substituting (30) into (5) and adding the resulting equation to (31), the multidimensional version of the semidiscretized TLS equation for the advection–diffusion equation is obtained:

$$\mathscr{A}_1 c^{n+1} = \mathscr{A}_2 c^n, \tag{32}$$

where

$$\mathscr{A}_1 = 1 + \alpha_1 \mathbf{u}\cdot\nabla + \alpha_2\{\mathbf{uu}:\nabla\nabla + [(\mathbf{u}\cdot\nabla)\mathbf{u}]\cdot\nabla\} - (\Delta t/2)[\nabla\cdot(\mathbf{D}\cdot\nabla)],$$
$$\mathscr{A}_2 = 1 + \beta_1 \mathbf{u}\cdot\nabla + \beta_2\{\mathbf{uu}:\nabla\nabla + [(\mathbf{u}\cdot\nabla)\mathbf{u}]\cdot\nabla\} + (\Delta t/2)[\nabla\cdot(\mathbf{D}\cdot\nabla)],$$

in which

$$\alpha_1 = \theta\Delta t, \qquad \beta_1 = -(1-\theta)\Delta t,$$
$$\alpha_2 = -(\Delta t^2/2)(\tfrac{1}{3} - \theta), \quad \beta_2 = (\Delta t^2/2)(\tfrac{2}{3} - \theta).$$

For unsteady flow, $\mathbf{u} = \mathbf{u}^{n+1}$ in $\mathscr{A}_1$ and $\mathbf{u} = \mathbf{u}^n$ in $\mathscr{A}_2$. Zero variation of the least-squares functional for (32) becomes

$$\int_\Omega d\Omega[\mathscr{A}_1 c^{n+1} - \mathscr{A}_2 c^n]\,\mathscr{A}_1 \delta c^{n+1} = 0. \tag{33}$$

Again, using shape functions for δc^{n+1}, a multidimensional TLS scheme for the advection–diffusion equation results.

In this study the accuracy of the multidimensional TLS scheme is demonstrated in two-dimensions. A set of non-conforming Hermite cubic basis functions on triangular elements[28] were selected:

$$c(x,y,t) = \sum_{i=1}^{3}\left(N_i c_i + FX_i\frac{\partial c_i}{\partial x} + FY_i\frac{\partial c_i}{\partial y}\right), \tag{34}$$

where

$$N_i = -\frac{y_j - y_k}{2A}\sum_{p=1}^{3} FX_p + \frac{x_j - x_k}{2A}\sum_{p=1}^{3} FY_p + L_i,$$
$$FX_i = L_i^2[-(x_i - x_j)L_j + (x_k - x_i)L_k] + \tfrac{1}{2}(-2x_i + x_j + x_k)L_1L_2L_3,$$
$$FY_i = L_i^2[-(y_i - y_j)L_j + (y_k - y_i)L_k] + \tfrac{1}{2}(-2y_i + y_j + y_k)L_1L_2L_3,$$

in which A is the area of a triangular element, (x_i, y_i) are the co-ordinates of the vertices, L_i is the area co-ordinate and the subscripts (i, j, k) are in cyclic order.

7. NUMERICAL EXAMPLES

The same types of example problems as in the one-dimensional case are chosen: advection of a Gaussian hill in a rotating flow field[27] and of a sharp front with linear velocity. The domain is a square with $x, y \in [-3400, 3400]$ and is discretized by 35×35 mesh. Each 200×200 subsquare is further divided by two triangular elements. For the Gaussian hill problem the flow field is given as

$$\begin{Bmatrix} u \\ v \end{Bmatrix} = \phi \begin{Bmatrix} -y \\ x \end{Bmatrix}, \tag{35}$$

where $\phi = \pi/1500$, and the initial condition is

$$c(x, y, 0) = \exp\left(-\frac{1}{2\sigma^2}[x^2 + (y + 1800)^2]\right),$$

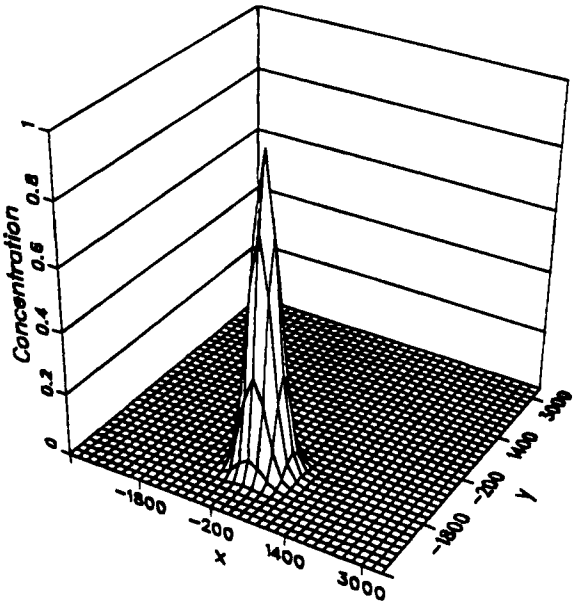

Figure 5. The Gaussian hill after one revolution; $\Delta x = \Delta y = 200$, $\Delta t = 15$

where $\sigma = 264$. Homogeneous Dirichlet boundary conditions are enforced at the inflow boundary. A time step $\Delta t = 15$ was used to avoid the Courant number exceeding unity at the corners. The result after one revolution is reported in Figure 5 and is impressive in that it indicates almost no numerical diffusion. The peak value is 0·984 and $c_{\min} = 0{\cdot}0$, i.e. less than 2% dissipation at the peak and no undershoot at all. Moreover, no nodal value has changed more than 2% from the initial condition. The superior behaviour of the TLS scheme can be demonstrated by doubling the spatial increments to 400. With this spacing the hill is distributed only over $4\Delta x$ in either direction, which is the minimum to describe a Gaussian hill. As a result, the number of nodes is reduced from 1225 to 289. The centre of the initial hill is moved to (0, −1600) and $\Delta t = 30$ is used. The result after one revolution is given in Figure 6. There appears more dissipation and a small magnitude of undershoot: $c_{\max} = 0{\cdot}829$ and $c_{\min} = -0{\cdot}018$. Leismann and Herrling[29] used a linear element Petrov–Galerkin method to solve the same problem with $\Delta x = \Delta y = 200$ and $\Delta t = 10$. For comparison, their peak was reduced to about 0·73 and $c_{\min} = -0{\cdot}05$. Also, the TLS scheme did much better in preserving the symmetry of the hill. Thus in this particular case the TLS method is capable of producing better results than the linear Petrov–Galerkin scheme while using a coarser grid which results in fewer unknowns and larger time increments.

For the sharp front problem the initial and boundary conditions are

$$c(x, y, 0) = 0$$

and

$$c = 1 \quad \forall t \quad \text{at} \quad x = -3400, \qquad y \in [-3400, 3400],$$
$$c = 0 \quad \forall t \quad \text{at} \quad x \in [-3400, 3400], \quad y = -3400$$

respectively. The differences in the examples are in the flow field: for the first case $u = v = 1$ so that the side of an advancing front always coincides with the sides of the elements, and for the second

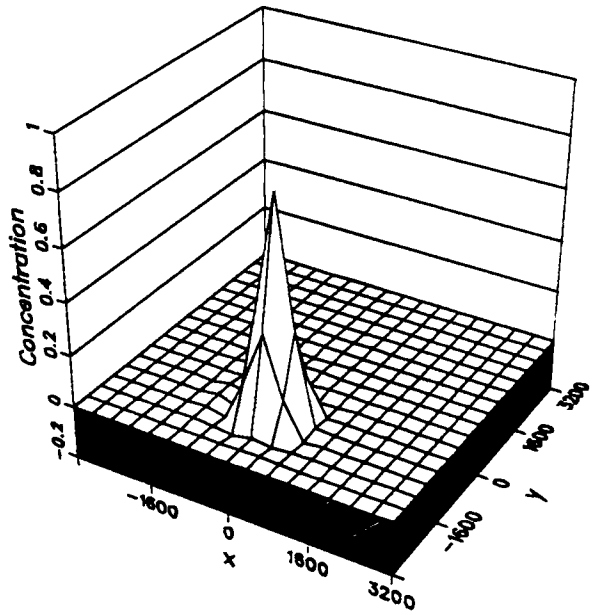

Figure 6. The Gaussian hill after one revolution; $\Delta x = \Delta y = 400$, $\Delta t = 30$

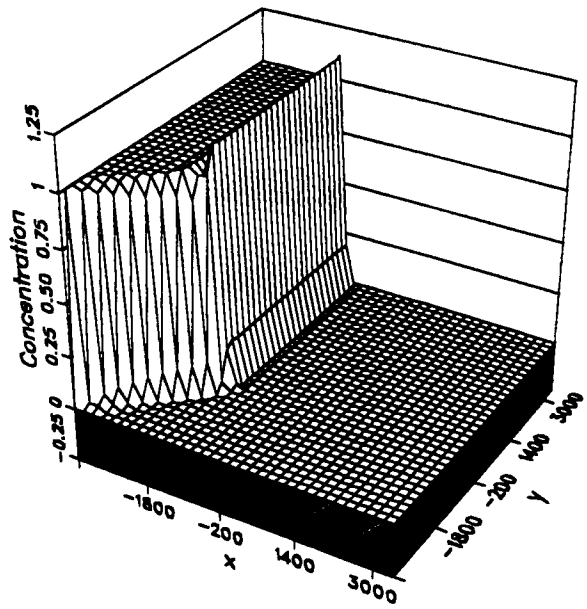

Figure 7. The sharp front at $t = 2000$ when $u = v = 1$

case $u = 2$ and $v = 1$ so that the side of the front falls inside the elements. The same discretization as with the first Gaussian hill problem is used. The results at $t = 2000$ using $\Delta t = 50$ are given in Figures 7 and 8 respectively. For the first case $c_{max} = 1{\cdot}113$ and $c_{min} = -0{\cdot}018$, and for the second problem $c_{max} = 1{\cdot}035$ and $c_{min} = -0{\cdot}026$. In both cases the spurious oscillations are confined

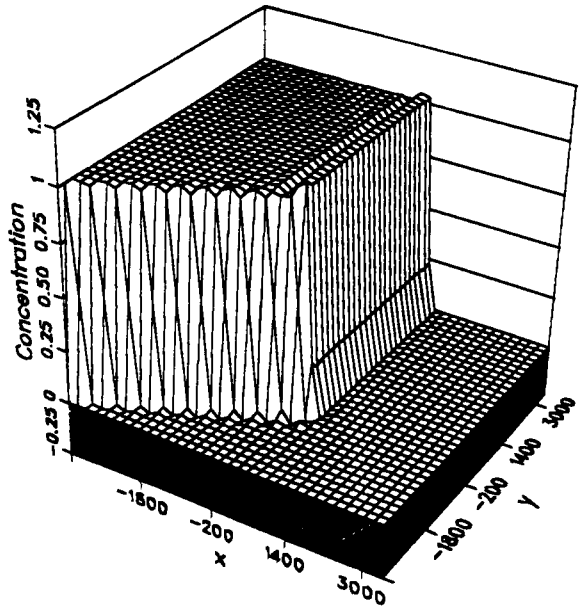

Figure 8. The sharp front at $t = 2000$ when $u = 2$, $v = 1$

within a few elements as in one-dimensional problems. Moreover, there is only small crosswind diffusion, a problem on which there has been extensive research in the Petrov–Galerkin method (e.g. References 11 and 12).

8. CONCLUSIONS

In this study the Taylor–least-squares (TLS) scheme is developed for numerical approximations of the advection-dominated unsteady advection–diffusion equation. The method offers direct generalizations to higher dimensions without losing the accuracy which was demonstrated in one dimension. The new scheme is compared with the Taylor–Galerkin[21] and least-squares[22] methods. TLS with Hermite cubic elements is shown to be superior to other methods by both Fourier analyses and numerical examples. Unlike the Petrov–Galerkin methods and other schemes, the TLS scheme does not present difficulties in extension to multidimensions in that it does not lose accuracy and is not subject to crosswind diffusion. Because the Hermite cubic element involves three degrees of freedom per node, the method can be computationally expensive. Fortunately, the scheme allows the use of coarse grids with good accuracy. A numerical example demonstrated that the TLS scheme behaves very well for a coarse discretization. Further work is needed to identify the theoretical stability criterion of the method, which was not obtained in this study owing to the complexity of the eigenvalues. However, Fourier analyses showed that the scheme can be stable up to the unit Courant number with a proper value of θ, though the accuracy degenerates as the Courant number approaches unity.

In this study the third-order Taylor scheme is used to discretize the advection–diffusion equation, which Donea *et al.*[20] had discretized only to second order owing to the diffusion term. Excellent agreement was obtained between analytic and numerical solutions.

ACKNOWLEDGEMENTS

This work was supported by a grant from the National Science Foundation (ECE-8610119) and conducted using the Cornell National Supercomputer Facility, a resource of the Center for Theory and Simulation in Science and Engineering (Theory Center), which receives major funding from the National Science Foundation and IBM Corporation with additional support from New York State and members of the Corporate Research Institute. The authors also would like to thank the reviewers for their valuable comments.

APPENDIX

All the coefficients in this appendix were obtained using MACSYMA.[30] For LWTG with the cubic elements

$$a = \frac{245v^4 + 556v^2 + 131}{3150} - \frac{1}{6300}[(280v^4 + 128v^2 + 72)(e^{\lambda} + e^{-\lambda}) + (-35v^4 + 8v^2 - 1)(e^{2\lambda} + e^{-2\lambda})],$$

$$b = \frac{490v^4 + 278v^2 - 131}{1575} - \frac{1}{3150}[(560v^4 - 280v^3 + 64v^2 + 192v - 72)e^{\lambda} + (560v^4 + 280v^3 + 64v^2 - 192v - 72)e^{-\lambda} + (-70v^4 + 35v^3 + 4v^2 - 6v + 1)e^{2\lambda} + (-70v^4 - 35v^3 + 4v^2 + 6v + 1)e^{-2\lambda}],$$

$$d = \frac{980v^4 - 146v^2 + 131}{3150} - \frac{1}{6300}[(1120v^4 - 1120v^3 + 752v^2 - 384v + 72)e^{\lambda} + (1120v^4 + 1120v^3 + 752v^2 + 384v + 72)e^{-\lambda} + (-140v^4 + 140v^3 - 58v^2 + 12v - 1)e^{2\lambda} + (-140v^4 - 140v^3 - 58v^2 - 12v - 1)e^{-2\lambda}].$$

For LS with the cubic elements

$$a = \frac{2205v^4 + 3336v^2 + 524}{12\,600} - \frac{1}{25\,200}[(2520v^4 + 768v^2 + 288)(e^{\lambda} + e^{-\lambda}) + (-315v^4 + 48v^2 - 4)(e^{2\lambda} + e^{-2\lambda})],$$

$$b = \frac{2205v^4 - 524}{6300} - \frac{1}{12600}[(2520v^4 - 1680v^3 + 768v - 288)e^{\lambda} + (-315v^4 + 210v^3 - 24v + 4)e^{2\lambda} + (2520v^4 + 1680v^3 - 768v - 288)e^{-\lambda} + (-315v^4 - 210v^3 + 24v + 4)e^{-2\lambda}],$$

$$d = \frac{2205v^4 + 528v^2 + 524}{12\,600}$$
$$- \frac{1}{25\,200}[(2520v^4 - 3360v^3 + 3264v^2 - 1536v + 288)e^{\lambda}$$
$$+ (-315v^4 + 420v^3 - 216v^2 + 48v - 4)e^{2\lambda}$$
$$+ (2520v^4 + 3360v^3 + 3264v^2 + 1536v + 288)e^{-\lambda}$$
$$+ (-315v^4 - 420v^3 - 216v^2 - 48v - 4)e^{-2\lambda}].$$

For the TLS scheme

$$a = \frac{175v^8 + 560v^6 + 2985v^4 + 1112v^2 + 524}{12\,600}$$
$$- \frac{1}{75\,600}[(700v^8 + 1540v^6 - 3600v^4 + 768v^2 + 864)(e^{\lambda} + e^{-\lambda})$$
$$+ (-175v^8 + 140v^6 - 45v^4 + 48v^2 - 12)(e^{2\lambda} + e^{-2\lambda})],$$

$$b = \frac{175v^8 - 1120v^6 + 1515v^4 - 2224v^2 + 524}{6300}$$
$$+ \frac{1}{37\,800}[(700v^8 - 1050v^7 - 3080v^6 + 7140v^5$$
$$- 8640v^4 + 7920v^3 - 1536v^2 - 2304v^2 + 864)e^{\lambda}$$
$$+ (-175v^8 + 525v^7 - 280v^6 - 420v^5 + 585v^4 - 180v^3 - 96v^2 + 72v - 12)e^{2\lambda}$$
$$+ (700v^8 + 1050v^7 - 3080v^6 - 7140v^5 - 8640v^4 - 7920v^3 - 1536v^2 + 2304v + 864)e^{-\lambda}$$
$$+ (-175v^8 - 525v^7 - 280v^6 + 420v^5 + 585v^4 + 180v^3 - 96v^2 - 72v - 12)e^{-2\lambda}],$$

$$d = \frac{175v^8 - 700v^6 + 1725v^4 - 1696v^2 + 524}{12\,600}$$
$$- \frac{1}{75\,600}[(700v^8 - 2100v^7 + 700v^6 + 4200v^5$$
$$- 3600v^4 - 4320v^3 + 8256v^2 + 4608v + 864)e^{\lambda}$$
$$+ (-175v^8 + 1050v^7 - 2800v^6 + 4200v^5 - 3825v^4 + 2160v^3 - 744v^2 + 144v - 12)e^{2\lambda}$$
$$+ (700v^8 + 2100v^7 + 700v^6 - 4200v^5 - 3600v^4 + 4320v^3 + 8256v^2 + 4608v + 864)e^{-\lambda}$$
$$+ (-175v^8 - 1050v^7 - 2800v^6 - 4200v^5 - 3825v^4 - 2160v^3 - 744v^2 - 144v - 12)e^{-2\lambda}],$$

where $\lambda = ik\Delta x$.

REFERENCES

1. H. S. Price, R. S. Varga and J. E. Warren, 'Application of oscillation matrices to diffusion convection equations', *J. Math. Phys.*, **45**, 301–311 (1966).
2. O. K. Jensen and B. A. Finlayson, 'Oscillation limits for weighted residual methods applied to convective diffusion equations', *Int. j. numer. methods eng.*, **15**, 1681–1689 (1980).

3. D. U. von Rosenberg, 'An explicit finite difference solution to the convection–dispersion equation', *Numer. Methods PDE*, **2**, 229–237 (1986).
4. P. Colella and P. R. Woodward, 'The piecewise parabolic method (PPM) for gas-dynamical simulations', *J. Comput. Phys.*, **54**, 174–201 (1984).
5. R. D. Richtmyer and K. W. Morton, *Difference Methods for Initial-Value Problems*, Interscience, 1967, pp. 338–345.
6. E. Varoglu and W. D. L. Finn, 'A finite element method for the diffusion–convection equation', in C. A. Brebbia, W. G. Gray and G. F. Pinder (eds), *Proc. II Int. Conf. on Finite Elements in Water Resources*, Imperial College, London, 1978, pp. 4.3–4.20.
7. J. B. Bell, C. N. Dawson and G. R. Shubin, 'An unsplit, higher order Godunov method for scalar conservation laws in multiple dimensions', *J. Comput. Phys.*, **74**, 1–24 (1988).
8. L. Demkowicz and J. T. Oden, 'An adaptive characteristic Petrov–Galerkin finite element method for convection-dominated linear and nonlinear parabolic problems in one space variable', *J. Comput. Phys.*, **67**, 188–213 (1986).
9. Ph. Devloo, J. T. Oden and P. Pattani, 'An h-p adaptive finite element method for the numerical simulation of compressible flow', *Comput. Methods Appl. Mech. Eng.*, **70**, 203–235 (1988).
10. I. Christie, D. F. Griffiths and A. R. Mitchell, 'Finite element methods for second order differential equations with significant first derivatives', *Int. j. numer. methods eng.*, **10**, 1389–1396 (1976).
11. T. J. R. Hughes and A. Brooks, 'A theoretical framework for Petrov–Galerkin methods with discontinuous weighting functions: application to the streamline-upwind procedure', in R. H. Gallagher, D. H. Norrie, J. T. Oden and O. C. Zienkiewicz (eds), *Finite Elements in Fluids, Vol. 4*, Wiley, 1982, pp. 47–65.
12. A. C. Galeão and E. G. Dutra Do Carmo, 'A consistent approximate upwind Petrov–Galerkin method for convection dominated problems', *Comput. Methods Appl. Mech. Eng.*, **68**, 83–95 (1988).
13. L. P. Franca, I. Harari, T. J. R. Hughes, M. Mallet, F. Shakib, T. E. Spelce, F. Chalot and T. E. Tezduyar, 'A Petrov–Galerkin finite element method for the compressible Euler and Navier–Stokes equations', in T. E. Tezduyar and T. J. R. Hughes (eds), *Numerical Methods in Computational Flows—Finite Difference, Element and Volume Techniques*, AMD, ASME, 1986, pp. 19–43.
14. F. M. Holly, Jr. and A. Priessmann, 'Accurate calculation of transport in two dimension', *J. Hydraul. Div., ASCE*, **103**, 1259–1277 (1977).
15. F. M. Holly, Jr. and J.-M. Usseglio-Polatera, 'Dispersion simulation in two-dimensional tidal flow', *J. Hydraul. Eng., ASCE*, **110**, 905–927 (1984).
16. D. Ding and P. L.-F. Liu, 'An operator-splitting algorithm for two-dimensional convection–dispersion–reaction problems', *Int. j. numer. methods eng.*, **28**, 1023–1040 (1989).
17. D. Ding and P. L.-F. Liu, 'An operator splitting algorithm for three dimensional convection–diffusion problems', unpublished manuscript, 1988.
18. P. L.-F. Liu, private communication, 1988.
19. K. W. Morton and A. K. Parrott, 'Generalised Galerkin methods for first order hyperbolic equations', *J. Comput. Phys.*, **36**, 249–270 (1980).
20. J. Donea, S. Giuliani, H. Laval and L. Quartapelle, 'Time-accurate solution of advection–diffusion problems by finite elements', *Comput. Methods Appl. Mech. Eng.*, **45**, 123–145 (1984).
21. J. Donea, L. Quartapelle and V. Selmin, 'An analysis of time discretization in the finite element solution of hyperbolic problems', *J. Comput. Phys.*, **70**, 463–499 (1987).
22. G. F. Carey and B. N. Jiang, 'Least-squares finite elements for first-order hyperbolic systems', *Int. j. numer. methods eng.*, **26**, 81–93 (1988).
23. A. E. Taigbenu, N.-S. Park, A. G. Ayala and J. A. Liggett, 'Remarks on the solution of the diffusion-advection equation', *Int. Conf. on Computational Methods in Flow Analysis*, Okayama, September 1988.
24. K. W. Morton, 'Generalised Galerkin methods for hyperbolic problems', *Comput. Methods Appl. Mech. Eng.*, **52**, 847–871 (1985).
25. L. Lapidus and G. F. Pinder, *Numerical Solutions of Partial Differential Equations in Science and Engineering*, Wiley–Interscience, 1982, pp. 67–72.
26. S. Bates and B. Cathers, 'Analysis of spurious eigenmodes in finite element equations', *Int. j. numer. methods. eng.*, **23**, 1131–1143 (1986).
27. A. M. Baptista, 'Reference problems for the convection–diffusion forum', *VI Int. Conf. on Finite Elements in Water Resources*, Lisbon, 1986.
28. G. Bazeley, Y. Cheung, B. Irons and O. C. Zienkiewicz, 'Triangular elements in plate bending–conforming and nonconforming solutions', *Proc. (First) Conf. on Matrix Methods in Structural Mechanics, AFFDL TR 66–80*, 1965, pp. 547–576.
29. H. M. Leismann and B. Herrling, 'Streamline-upwind/Petrov–Galerkin method with an increased order of consistence', *VI Int. Conf. on Finite Elements on Water Resources*, Lisbon, 1986.
30. R. H. Rand and D. Armbruster, *Perturbation Methods, Bifurcation Theory and Computer Algebra*, Springer- Verlag, 1987, pp. 215–233.